Forty-five years of cGMP research in *Dictyostelium*: understanding the regulation and function of the cGMP pathway for cell movement and chemotaxis

Peter J. M. van Haastert*, Ineke Keizer-Gunnink, Henderikus Pots, Claudia Ortiz-Mateos, Douwe Veltman, Wouter van Egmond, and Arjan Kortholt
Department of Cell Biochemistry, University of Groningen, 9747 AG Groningen, the Netherlands

ABSTRACT **In *Dictyostelium*, chemoattractants induce a fast cGMP response that mediates myosin filament formation in the rear of the cell. The major cGMP signaling pathway consists of a soluble guanylyl cyclase sGC, a cGMP-stimulated cGMP-specific phosphodiesterase, and the cGMP-target protein GbpC. Here we combine published experiments with many unpublished experiments performed in the past 45 years on the regulation and function of the cGMP signaling pathway. The chemoattractants stimulate heterotrimeric Gαβγ and monomeric Ras proteins. A fraction of the soluble guanylyl cyclase sGC binds with high affinity to a limited number of membrane binding sites, which is essential for sGC to become activated by Ras and Gα proteins. sGC can also bind to F-actin; binding to branched F-actin in pseudopods enhances basal sGC activity, whereas binding to parallel F-actin in the cortex reduces sGC activity. The cGMP pathway mediates cell polarity by inhibiting the rear: in unstimulated cells by sGC activity in the branched F-actin of pseudopods, in a shallow gradient by stimulated cGMP formation in pseudopods at the leading edge, and during cAMP oscillation to erase the previous polarity and establish a new polarity axis that aligns with the direction of the passing cAMP wave.**

Monitoring Editor
Leah Edelstein-Keshet
University of British Columbia

Received: Apr 6, 2021
Revised: Jul 15, 2021
Accepted: Jul 30, 2021

INTRODUCTION

Chemotaxis is important for *Dictyostelium* cells as it helps the cells to find food using secretion products of bacteria, their prey (Konijn, 1969). It also helps them to survive periods of food deprivation when they aggregate by means of chemotaxis to compounds secreted by themselves (Bonner, 1947). In the multicellular structure, cell movement organizes the tissue into regions of prestalk and prespore cells guided by morphogens inducing chemotaxis and cell-type–specific gene expression (Schaap *et al.*, 1984; Bretschneider *et al.*, 1995). Some chemoattractants secreted by bacteria have been identified as folate and pterins, but probably several still have to be characterized (Pan *et al.*, 1972). The chemoattractants used for cell aggregation are partially species specific. The most widely studied species, *Dictyostelium discoideum*, uses cAMP as chemoattractant (Konijn *et al.*, 1967), while *Dictyostelium lacteum* uses a pterin derivative (Van Haastert *et al.*, 1982b), *Dictyostelium minutum* a folate derivative (de Wit and Konijn, 1983), and *Polysphondylium violaceum* a dipeptide (Shimomura *et al.*, 1982). About 45 years ago it was discovered that cGMP is produced intracellularly upon stimulation of cells with a chemoattractant. Probably the first experiment was performed with the not-yet-characterized chemoattractant for *D. lacteum* purified from yeast extract (Mato and Konijn, 1977). For *D. discoideum*, which uses cAMP as chemoattractant, it was known that cAMP induces the intracellular increase of cAMP, which is subsequently secreted. The aim of the experiment with *D. lacteum* was

This article was published online ahead of print in MBoC in Press (http://www.molbiolcell.org/cgi/doi/10.1091/mbc.E21-04-0171).

Conflict of interest: The authors declare no conflict of interest.

Author contributions: P.J.M.v.H., D.V., W.v.E., and A.K. designed the experiments. P.J.M.v.H., I.K.-G., H.P., C.O.-M., D.V., and W.v.E. performed the experiments. P.J.M.v.H., I.K.-G., D.V., W.v.E., and A.K. analyzed the data. P.J.M.v.H. and A.K. wrote the manuscript, and all authors approved it before submission.

*Address correspondence to: Peter J. M. van Haastert (P.J.M.van.Haastert@rug.nl).

Abbreviations used: EGTA, ethylene glycol-bis(β-aminoethyl ether)-*N,N,N′,N′*-tetraacetic acid; GC, guanylyl cyclase; GFP, green fluorescent protein; GPCR, G-protein coupled receptor; PB, 10 mM phosphate buffer; RBD, Ras binding domain.

Condition	GCA (% of sum)	sGC (% of sum)
1 h starved		
Enzyme activity (pmol/min per mg)	5.8 ± 1.7 (35%)	11.0 ± 1.1 (65%)
cGMP response by folate (pmol/10^7 cells)	1.8 ± 0.4 (18%)	8.5 ± 1.5 (82%)
5 h starved		
Enzyme activity (pmol/min per mg)	2.6 ± 0.6 (13%)	17.1 ± 2.2 (87%)
cGMP response by cAMP (pmol/10^7 cells)	1.5 ± 1.2 (7%)	18.7 ± 3.4 (93%)

sgc-null and *gca*-null cells express only GCA or only sGC, respectively. Cells were starved for 1 h or 5 h to make them optimally sensitive to folate and cAMP, respectively. Guanylyl cyclase enzyme activity was measured in cell lysates using Mg^{2+}-GTP as substrate. Intact cells were stimulated with either 1 μM folate or 0.1 μM cAMP, and samples for cGMP determination were collected at 0 and 10 s after stimulation; the increase of cGMP levels at 10 s after stimulation is shown. Data are means and SD of three independent experiments, each with triplicate determinations. The relative importance of GCA and sGC in enzyme activity and cGMP responses is calculated as percentage of the sum of the activities.

TABLE 1: Contribution of GCA and sGC to guanylyl cyclase activity and chemoattractant-stimulated cGMP response.

to see whether a species that does not use cAMP as chemoattractant uses cAMP as second messenger. The result was negative; no increase of cAMP levels was detected. Because the samples were already present, the levels of cGMP were determined, demonstrating a very fast and strong increase of cGMP levels. Soon thereafter it was shown that a similar cGMP response was induced by the chemoattractant cAMP in *D. discoideum* (Mato *et al.*, 1977; Wurster *et al.*, 1977) and by the dipeptide in *P. violaceum* (De Wit *et al.*, 1988). Interestingly, a few years later it was shown that many chemoattractants that do not induce cAMP levels during aggregation do induce a cAMP increase during multicellular development (Schaap and Wang, 1984, 1985; Schaap *et al.*, 1984). The first 25 years of cGMP research has been reviewed by Bosgraaf and Van Haastert (2002). This review describes for *D. discoideum* the identification and biochemical characterization of the guanylyl cyclases, cGMP-binding proteins, and cGMP-phosphodiesterases, the regulation of these enzymes in signal transduction pathways, the characterization of several mutants defective in one of these enzymes or their regulation, and finally the cloning of the genes encoding the relevant enzymes.

The cGMP system in *D. discoideum* consists of two guanylyl cyclases, GCA with the topology of a membrane-bound adenylyl cyclase with 12 transmembrane segments (Roelofs *et al.*, 2001c) that is always membrane bound and sGC with the topology of a soluble adenylyl cyclase that is found in the cytosol and is slightly enriched at the boundary of the cell (Roelofs *et al.*, 2001b). GCA and sGC are both activated by the extracellular chemoattractants folate and cAMP, but sGC has the largest contribution (Roelofs and Van Haastert, 2002). The cGMP produced is mainly degraded by a cGMP-stimulated cGMP-specific phosphodiesterase (GbpA, PDE5, or PdeD, product of the *stmF* locus) (Van Haastert *et al.*, 1982a; Bosgraaf *et al.*, 2002b; Meima *et al.*, 2002). Minor contributions are by the high-affinity cGMP-specific PDE3 (about 10%) and by secretion followed by extracellular degradation by the nonspecific PDE1 (about 10%) (Bader *et al.*, 2007). The cGMP produced can also bind and activate its high-affinity target, GbpC (Bosgraaf *et al.*, 2002a). No evidence is available for other functional cGMP targets in *Dictyostelium*. In *gbpC*-null cells all high-affinity (4 nM) binding is lost, unveiling a low-affinity (300 μM) cGMP-binding protein (Bosgraaf *et al.*, 2002a; Van Egmond, 2010). This protein was purified and identified as nucleotide diphosphokinase (NDPK) (Van Egmond, 2010): millimolar concentrations of ATP, ADP, GTP, and GDP compete with [^{3}H]-cGMP binding to the low-affinity cGMP-binding protein in *gbpC*-null cells, and submillimolar concentrations of cGMP act as competitive inhibitors of the NDPK enzymatic activity (ATP + GDP → ADP + GTP) (Van Egmond, 2010); because cGMP may mimic GDP, and because cGMP does not reach these high concentration, we consider NDPK as not a relevant functional cGMP target. Therefore, the main players are the guanylyl cyclase sGC, the phosphodiesterase PDE5, and the cGMP-target GbpC.

In the past 20 years many experiments have been performed on the regulation of these enzymes using the cloned genes. These experiments include localization with green fluorescent protein (GFP)-tagged proteins, functional studies with null mutants, and investigating specific regulatory processes by expressing mutated proteins. Here we combine published and many unpublished experiments on the regulation and function of this chemoattractant-stimulated cGMP pathway.

RESULTS

Activation of sGC by cAMP/folate in vivo and by GTPγS in vitro

Major contribution of sGC. *Dictyostelium* has two guanylyl cyclase, GCA and sGC (Roelofs *et al.*, 2001c,b). GCA has the predicted topology of a membrane-bound adenylyl cyclase with 12 transmembrane-spanning domains and is present only in the membrane fraction of a cell lysate. sGC has the predicted topology of a soluble adenylyl cyclase and is localized in the cytosol but also at the boundary of the cell where the plasma membrane and cortical F-actin are present. GCA is expressed maximally during growth and multicellular development, whereas sGC is expressed maximally during starvation (Roelofs and Van Haastert, 2002). The properties of GCA and sGC were investigated in two cell lines: sGC is the only guanylyl cyclase in *gca*-null cells, while *sgc*-null cells express only GCA (Roelofs and Van Haastert, 2002). Here we analyzed these data to establish the relative contribution of GCA and sGC to enzyme activity and cGMP response (Table 1). Although GCA has its highest activity in growing and 1-h-starved cells, its contribution to the total GC activity is only 35% (Table 1). The contribution of GCA to the folate-stimulated cGMP response is still smaller, only 18%, and sGC provides by far the largest contribution to the folate-stimulated cGMP response. In 5-h-starved cells, the activity of GCA has declined and it contributes 13% to the total GC activity and just 7% to the cAMP-mediated cGMP response. The results in Table 1 indicate that in 1-h- and 5-h-starved cells, sGC always is the major contributor to guanylyl cyclase enzyme activity in vitro and chemoattractant-stimulated cGMP response in vivo. In the next Results sections, the large effects observed are interpreted as being mediated by sGC; in the *Discussion*, the potential contribution of GCA in some of the small effects observed is evaluated.

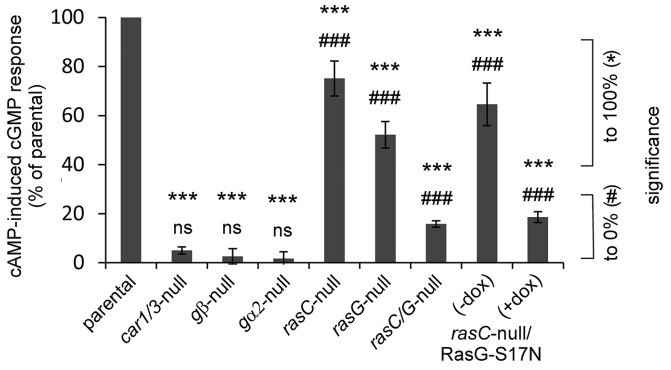

FIGURE 1: Stimulation of sGC in vivo by cAMP. The increase of cGMP levels at 10 s upon stimulation of the mutant is presented as % relative to the increase of cGMP levels upon stimulation of the parental strain of that mutant. The dominant negative RasG-S17N was expressed in *rasC*-null cells under the control of an inducible promotor that is activated by doxycycline (dox). Data are the means and SEM of two to nine experiments with triplicate determinations. Significance: *, different from response in control; #, different from 0; * or #, significant at $P < 0.05$; ** or ##, significant at $P < 0.01$; *** or ###, significant at $P < 0.001$; ns, not significant at $P > 0.05$.

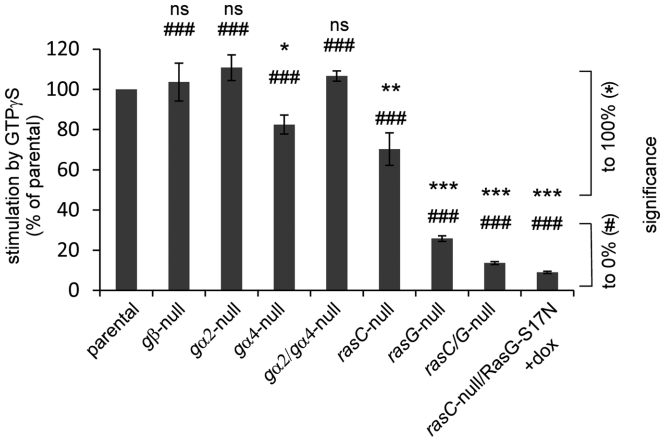

FIGURE 2: Stimulation of sGC in vitro by GTPγS. Guanylyl cyclase was measured in lysates with Mg^{2+}-GTP in the absence or presence of 50 µM GTPγS. The increase of activity by GTPγS in the mutant is presented as % relative to the increase by GTPγS in the parental strain of that mutant (see *Materials and Methods* for definition). Data are the means and SEM of two to five experiments with triplicate determinations. See Figure 1 caption for indications of significance.

Activation of sGC by cAMP in vivo requires Gα2βγ and Ras. The cAMP-induced cGMP accumulation after stimulation of starved *Dictyostelium* cells has been investigated in several signaling mutants. The results are presented as the increase of cGMP levels in the mutant relative to the increase of cGMP levels of the parental strain of that mutant (Figure 1). Null mutants of *cAR1/3*, *gα2*, and *gβ* do not exhibit a cAMP-induced cGMP increase, indicating that the cAMP receptors cAR1/3 and the heterotrimeric G-protein subunits Gα2 and Gβγ are essential components of the signaling pathway (Kesbeke *et al.*, 1988; Kumagai *et al.*, 1989, 1991; Sun *et al.*, 1990; Wu *et al.*, 1995; Kuwayama and Van Haastert, 1998b). The role of the monomeric Ras family members is more complex: The cGMP response is 75 ± 7% in *rasC*-null cells and 52 ± 6% in *rasG*-null cells relative to the response of their parental strain JH10 (Bolourani *et al.*, 2006, 2008) (mean and SEM). These responses are both statistically significant above 0% and significant below 100% ($P < 0.001$). The cGMP response of *rasC/rasG*-null cells is only 15.8 ± 1.2%. It should be noted that this strain is difficult to use because it has growth and developmental defects with reduced expression cAR1 and Gα2 (Bolourani *et al.*, 2006). Furthermore, the strain is unstable because it recovers wild-type properties after culture for a few weeks, probably due to the premature and enhanced expression of RasD (Khosla *et al.*, 2000; Bolourani *et al.*, 2010; Chattwood *et al.*, 2014). Therefore, we have measured the cGMP response in *rasC*-null cells expressing the dominant negative RasG-S17N from a tetracycline-inducible expression system that is activated by doxycycline (+Dox) (Veltman *et al.*, 2009b). We previously have shown that these cells expressing the dominant negative RasG-S17N do not show Ras activation upon cAMP stimulation as measured with the sensor Raf-RBD-GFP (Kortholt *et al.*, 2013). The results show that without induction the cGMP response is similar to that of *rasC*-null cells. Upon induction of RasG-S19N expression, the cGMP response of the obtained *rasC*-null/RasG-S17N cells is only 18 ± 2%. The results suggest that besides the heterotrimeric Gα2βγ a small G-protein is required to activate sGC. Both RasC and RasG can fulfill this role. Because the small cGMP response of *rasC*-null/RasG-S17N is still significant above 0, probably other small G-proteins such as RasD may contribute to the response in the absence of RasC and RasG. Together the data suggest that the cAMP-mediated cGMP signaling pathway in vivo is predominantly cAMP → cAR1/3 → Gα2βγ → RasC/G → sGC → cGMP.

Regulation of sGC in vitro by GTPγS in cell lysates is mediated by Ras. sGC in vitro is active with Mn^{2+}-GTP and Mg^{2+}-GTP as substrate (Janssens *et al.*, 1989; Schulkes *et al.*, 1992). Based on the required millimolar concentrations of Mn^{2+} and Mg^{2+} in combination with the cellular concentration of 10 µM Mn^{2+} versus 3 mM Mg^{2+}, it was concluded that Mg^{2+}-GTP is the physiological substrate (Janssens *et al.*, 1989; Roelofs and Van Haastert, 2002). The Mg^{2+}-GTP–dependent guanylyl cyclase activity is activated by micromolar concentrations of GTPγS, resembling the mode of action of heterotrimeric or monomeric GTP-binding proteins (Janssens *et al.*, 1989). The GTPγS-mediated activation of guanylyl cyclase activity in vitro has been investigated in several signaling mutants. The results are presented as the fold activation by GTPγS in the mutant relative to the fold activation by GTPγS in the parental strain of that mutant (Figure 2). GTPγS-mediated activation of sGC is normal in cell lysates prepared from *gβ*-null, *gα2*-null, *gα4*-null, and *gα2/gα4*-null cells, suggesting that heterotrimeric G-proteins do not mediate the effect of GTPγS (Wu *et al.*, 1995; Roelofs *et al.*, 2001a). Activation of sGC by GTPγS is still 70 ± 8% in lysates from *rasC*-null and 26 ±2 % in lysates from *rasG*-null cells (Bolourani *et al.*, 2008). However, activation by GTPγS is strongly reduced to 14 ± 1% in lysates from *rasC/rasG*-null cells (Bolourani *et al.*, 2008) and to only 9 ± 0.5% in lysates from *rasC*-null with induction of the dominant negative RasG-S17N (*rasC*-null/RasG-S17N + Dox; Figure 2).

Regulation of sGC in vitro by reconstitution with purified proteins. To directly establish the regulation of sGC in vitro, a lysate of wild-type cells containing sGC was incubated with purified and stable GTP-binding proteins. In this lysate GTPγS stimulates sGC activity 55% (Figure 3). Purified active Gα4-GppNHp has no effect on sGC activity. Purified Gβγ also does not activate the enzyme and even slightly but significantly inhibits sGC activity. Purified active Rap1-GppNHp has no effect. Importantly, purified active RasG-GppNHp stimulates sGC activity to a similar level as GTPγS, whereas

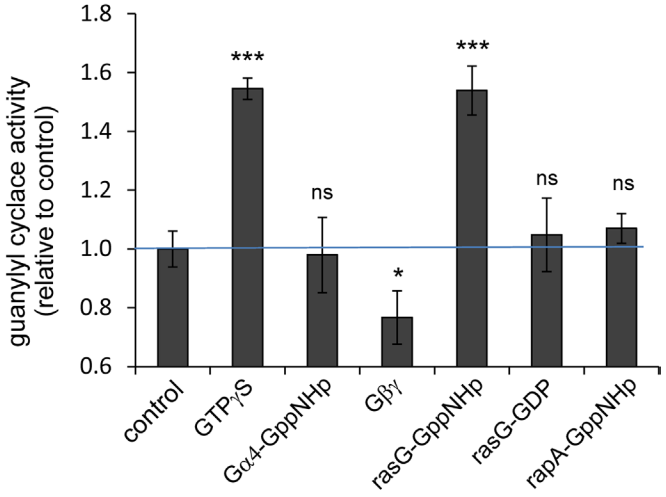

FIGURE 3: Reconstitution of sGC with purified proteins. A lysate from wild-type AX3 cells was reconstituted with the indicated purified protein for 60 s on ice and then assayed for guanylyl cyclase activity at room temperature. The activity is presented relative to the control without purified protein or GTPγS added. The data shown are the means and SEM of 12 (control) or four (all others) independent reconstitutions with triplicate time points. Significance: different from control at *, $P < 0.05$ or ***, $P < 0.001$; ns, not significant at $P > 0.05$.

the inactive RasG-GDP does not activate the enzyme. Unfortunately, we were not able to purify Gα2-GppNHp and RasC-GppNHp in a stable form.

The combined experiments with mutants and reconstitutions strongly suggest that GTPγS stimulation of sGC activity is mediated predominantly by RasG and partly by RasC, whereas heterotrimeric G-proteins do not have a direct effect on sGC activity. This suggests that the cAMP-mediated activation of sGC in vivo is a two-step reaction: first the activation of RasG and RasC by cAMP, which absolutely requires cAR1/3 and Gα2βγ, and the activation of sGC by activated RasG/RasC.

Ras activation by cAMP or folate in vivo is not sufficient for sGC activation. In *Dictyostelium*, Ras proteins are present uniformly at the plasma membrane as was deduced from the localization of GFP-RasG (Sasaki *et al.*, 2004). Stimulation of cells with cAMP does not change this localization of Ras but converts Ras from the inactive Ras-GDP state into active Ras-GTP. This activation can be measured with the sensor RBD-Raf-GFP. The RBD domain of mammalian Raf binds specifically to the GTP form of Ras, mainly RasG. Upon cAMP stimulation, free RBD-Raf-GFP in the cytoplasm translocates to the cell boundary, where it binds to Ras-GTP. As mentioned above, the activation of sGC in vivo is absent in *gα2*-null and *gβ*-null cells (Kesbeke *et al.*, 1988; Kumagai *et al.*, 1989; Wu *et al.*, 1995; Kuwayama and Van Haastert, 1998b). Interestingly, cAMP induces a partial activation of Ras in *gα2*-null cells: RBD-Raf-GFP shows a significant, fast, and transient translocation from the cytoplasm to the plasma membrane in cAMP-stimulated *gα2*-null cells (Kortholt *et al.*, 2013). We have carefully explored here the responses of *gα*-null and *gβ*-null cells. The Ras response in *gα2*-null cells is about 55% of the response in wild-type cells (Table 2). In addition, cAMP induces a significant 18% stimulation of F-actin in *gα2*-null cells as measured with the sensor LimE-GFP (Table 2). In contrast, the increase of cGMP levels in *gα2*-null cells is undetectable, indicating that it is less than 5% compared with the response of wild-type cells. Importantly, none of these cAMP-induced responses is significant in *gβ*-null cells (Table 2).

Vegetative cells are chemotactic to folate, which is detected by the folate receptor fAR1 and mediated by Gα4βγ (Hadwiger *et al.*, 1994; Pan *et al.*, 2016). Folate does not induce a cGMP response in *gα4*-null and *gβ*-null cells (Hadwiger *et al.*, 1994; Pan *et al.*, 2018). However, the Ras activation (Kataria *et al.*, 2013) and F-actin formation by folate are essentially normal in *gα4*-null cells (about 95% of those of wild type; see Table 2). In *gβ*-null cells folate does not induce Ras activation, F-actin formation, or a cGMP response.

Figure 1 reveals that the cAMP-induced cGMP response in vivo is strongly diminished in *rasG*-null cells, while Figure 3 shows that active RasG can activate sGC in vitro. To directly test whether RasG activation in vivo is sufficient for the activation of guanylyl cyclase, we expressed dominant active RasG-G12V under a tetracycline-inducible promotor in wild-type cells. The results reveal that upon induction of RasG-G12V expression, basal cGMP levels and cAMP-stimulated cGMP levels do not change: basal cGMP levels are 0.68 ± 0.12 pmol/10^7 cells after induction of RasG-G12V and 0.79 ± 0.21 pmol/10^7 cells before induction; cAMP-stimulated cGMP levels are 12.66 ± 5.21 pmol/10^7 cells after induction of RasG-G12V and 14.81 ± 4.97 pmol/10^7 cells before induction. In contrast to the absence of an effect of dominant RasG-G12V on the cGMP response, the similar dominant active RasG-G12T exhibits increased PI3K activation and protrusions (Sasaki *et al.*, 2004; Zhang *et al.*, 2008).

These results lead to several conclusions. First, Gα2 for cAMP and Gα4 for folate are not essential for Ras activation, but Gβγ is

Strain	Stimulus	Raf-RBD-GFP/Ras	LimE-GFP/F-actin	cGMP response
WT	cAMP	100 (12)	100 (12)	100 (6)
gβ-null	cAMP	8.1 ± 8.4 (4) NS	3.9 ± 7.1 (4) NS	2.6 ± 4.5 (3) NS
gα2-null	cAMP	55.3 ± 21.3 (6)	19.2 ± 10.0 (9)	1.7 ± 4.0 (9) NS
WT	Folate	100 (16)	100 (8)	100 (6)
gβ-null	Folate	3.3 ± 23.3 (4) NS	–5.0 ± 30 (4) NS	2.3 ± 6.1 (3) NS
gα4-null	Folate	92.7 ± 41.1 (16)	94.9 ± 16.2 (13)	3.1 ± 9.9 (3) NS

Starved cells were stimulated with 0.1 μM cAMP and vegetative cells with 1 μM folate. The depletion of Raf-RBD-GFP and LimE-GFP in the cytosol was measured as indicator for the activation of Ras and F-actin, respectively. The response in the mutants is presented as the % stimulation in the mutant relative to the % stimulation of the parental wild type (WT) run in parallel. The data are the means and SD with *n* in parentheses the number of experiments. For Ras and F-actin response, *n* in parentheses refers to the number of cells analyzed in two independent experiments. For cGMP response, *n* in parentheses refers to the number of independent experiments with triplicate determinations. Data in green, the response is significant above 0 at $P < .0.01$; data in purple, the response is not significant (NS) above 0 at $P > 0.05$. It appeared to be difficult to obtain many transformants in *gβ*-null cells, explaining the low number of cells analyzed.

TABLE 2: Activation of Ras, F-actin, and sGC in vivo in G-protein mutants.

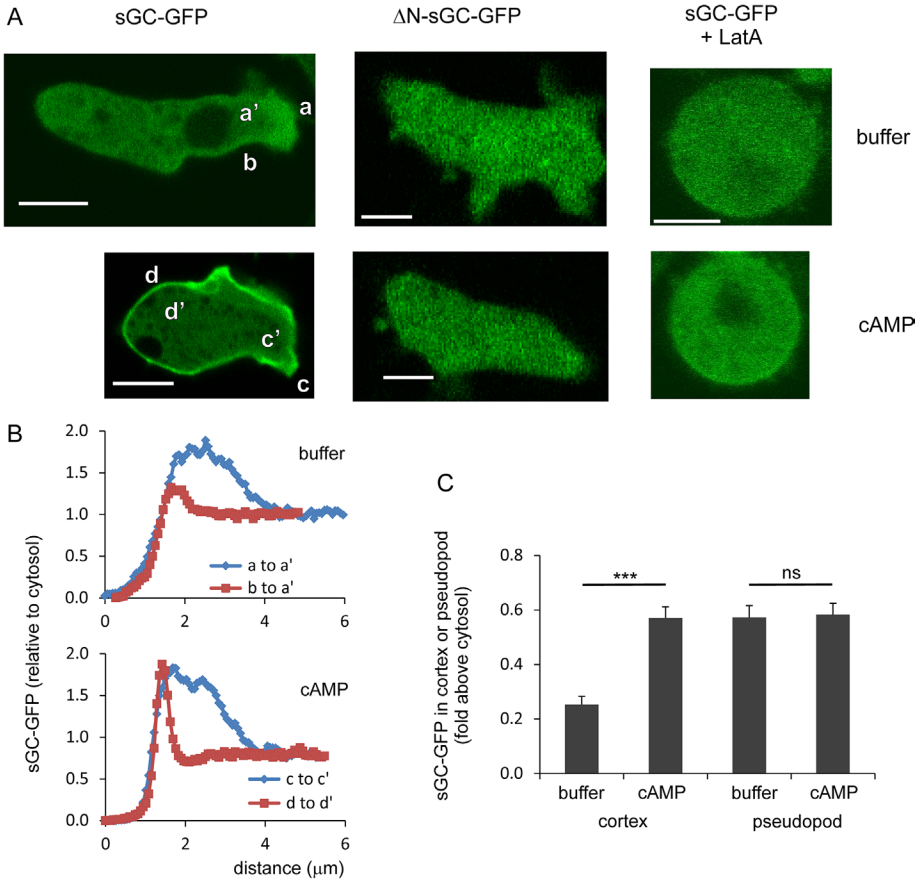

FIGURE 4: Localization of sGC-GFP in the cytoskeleton in pseudopods and the cortex. (A) Typical images of cells in buffer and at 10 s after stimulation with uniform 100 nM cAMP. Scale bars = 5 μm. (B) Quantification of sGC-GFP in buffer along the lines a to a′, b to a′, and after cAMP stimulation along the lines c to c′ and d to d′. Presented is the fluorescence intensity along the lines relative to the fluorescence intensity of the cytosol before stimulation. (C) sGC-GFP levels in the cortex at the boundary of the cell and in pseudopods of wild-type AX3 cells in buffer and after cAMP stimulation. The data shown are normalized to the GFP intensity of the cytosol before stimulation and are means and SEM with 14 cells analyzed. ***, significantly different at $P < 0.001$; ns, not significant at $P > 0.1$.

essential. cAMP activates besides Gα2βγ also Gα1βγ and Gα9βγ (Kumagai *et al.*, 1989; Bominaar and Van Haastert, 1994; Dharmawardhane *et al.*, 1994; Brzostowski *et al.*, 2002; Kataria *et al.*, 2013), and folate activates besides Gα4βγ also Gα5βγ (Hadwiger *et al.*, 1994; Hadwiger, 2007). This suggests that Ras activation is mediated by the subunit Gβγ that is released in small amounts from Gα1βγ or Gα9βγ in cAMP-stimulated *gα2*-null cells or is released in larger amounts from Gα5βγ in folate-stimulated *gα4*-null cells. Second, Ras activation in *gα2*-null and *gα4*-null cells is not sufficient for sGC activation. This suggests that sGC activation requires an activated Ras protein *and* an activated Gα subunit.

Interaction of sGC with the cytoskeleton

Localization of sGC-GFP in the cytoskeleton. In cells sGC-GFP is localized partly at the boundary of the cell, partly in protrusions, and mainly in the cytosol (Figure 4A). Upon the addition of the F-actin inhibitor latrunculin A (LatA) sGC-GFP becomes cytosolic, suggesting that sGC-GFP is enriched in the branched F-actin of pseudopods and the parallel F-actin of the contractile cortex immediately under the plasma membrane (Veltman *et al.*, 2005; Veltman and Van Haastert, 2006). Recently we observed (Van Haastert, 2020) that branched F-actin and parallel F-actin may have very different functions in the regulation of pseudopods and cell movement (see also Davidson and Wood, 2016; Rottner *et al.*, 2017). Therefore, the localization of sGC-GFP was quantified in detail in pseudopods and the cortex (Figure 4, B and C). In unstimulated starved wild-type cells, sGC-GFP in pseudopods and the cortex is about 0.57- and 0.25-fold above sGC-GFP in the cytosol, respectively. Upon stimulation with cAMP, the sGC-GFP intensity in pseudopods does not change significantly, while the sGC-GFP intensity in the cortex increases about twofold from 0.25 to 0.57, all relative to the sGC-GFP intensity in the cytosol before stimulation (Figure 4C). This increase of sGC-GFP in the cytoskeleton is associated with a 21% decrease of sGC-GFP in the cytosol (Veltman *et al.*, 2005; Veltman and Van Haastert, 2006; see also Figure 5 kinetics). In LatA, cAMP does not induce any detectable increase of sGC-GFP localization in the cortex or a detectable depletion from the cytosol (Figure 4A; Veltman and Van Haastert, 2006).

The association of sGC to the cytoskeleton requires the N-terminal segment. The truncation ΔN-sGC-GFP is cytosolic and not enriched in pseudopods or in the F-actin cortex at the boundary of the cell (Figure 4A; Veltman and Van Haastert, 2006). Conversely, the N-terminal segment fused to GFP ($N^{1\text{-}1010}$-sGC-GFP) is localized in pseudopods and at the boundary (Veltman and Van Haastert, 2006), indicating that this N-terminal segment is essential and sufficient for the localization of sGC in the cytoskeleton.

Kinetics of sGC activation and translocation to the cytoskeleton. Stimulation of cells with cAMP leads to the rapid translocation of sGC-GFP to the cortex, where it is in the vicinity of the plasma membrane containing the activators Gα2 and RasC/G. To understand the role of sGC-GFP translocation to the cortex for its activation, we measured the kinetics of this translocation in relation to the kinetics of sGC activation. For sGC activation, we reused the original data on the increase of cGMP levels at a very short time after cAMP stimulation (Van Haastert, 1987). This reveals that the increase of cGMP levels is constant between 1.5 and 7 s after stimulation with cAMP (Figure 5A); the onset time of the cGMP increase is $\tau = 0.85 \pm 0.32$ s after stimulation with cAMP (optimal value and 95% confidence level of the linear fit of cGMP levels; Figure 5C). sGC activity is proportional to the increase of cGMP levels (dcGMP/dt); this indicates that sGC is fully activated at 2 s after the addition of cAMP and that activation of sGC has an onset time of $\tau = 0.81 \pm 0.45$ s (Figure 5, A and C). Translocation of sGC-GFP to the cortex was measured as the depletion of sGC-GFP from the cytoplasm, because these measurements are very robust and sensitive (Veltman and Van Haastert, 2006). The depletion of sGC-GFP from the cytoplasm is relatively slow: it starts at $\tau = 3.38 \pm 0.51$ s after cAMP

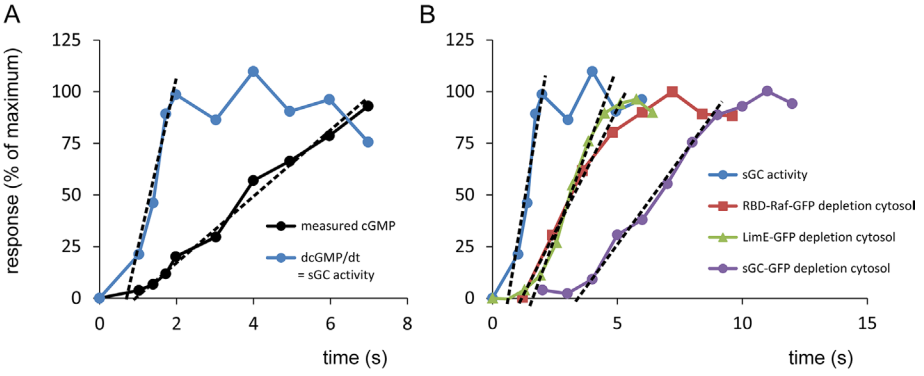

C

process	detection	units	Response time τ (s)	minus 0.75s delay
cGMP increase	cGMP	pmol/10^7 cells	0.85 ± 0.32	
sGC activation	d(cGMP)/dt	pmol/s/10^7 cells	0.81 ± 0.45	
Ras activation	RBD-Raf-GFP	% depletion cytosol	1.15 ± 0.49	0.40 ± 0.49
F-actin formation	LimE-GFP	% depletion cytosol	1.68 ± 0.43	0.93 ±0.43
association sGC to F-actin	sGC-GFP	% depletion cytosol	3.38 ± 0.51	

FIGURE 5: Kinetics of cGMP-related responses. (A, B) Kinetics of the responses. Prestimulus levels are set at 0% and the maximal response at 100%. The data between 10% and 75% were subjected to linear regression. The intersection with the *x*-axis is τ, the onset time of the response in seconds. (C) Table showing the optimal values of τ and the 95% confidence levels. The cGMP response, sGC activity, and sGC-GFP translocations are real-time determinations. In contrast, Ras activation and the formation of F-actin are indirect measurements using sensors that translocate from cytosol to the boundary of the cell. These indirect assays have a delay that is estimated to be 0.75 s (see Supplemental Figure S1).

stimulation (Figure 5, B and C). Thereby, translocation of sGC-GFP to the cytoskeleton occurs well after activation of sGC. We conclude that translocation of sGC-GFP to the cortex near the plasma membrane is not involved in the activation of sGC-GFP by membrane-localized Ras and Gα2.

In these experiments we also collected kinetic data on the activation of Ras and the formation of F-actin. The activation of Ras and the formation of F-actin cannot be monitored in real time directly but was measured by specific sensors: RBD-Raf-GFP for the active Ras-GTP (Kortholt *et al.*, 2013) and LimE-GFP for both branched and parallel F-actin (Kamp, 2019). The results reveal that depletion of RBD-Raf-GFP occurs rapidly with an onset time of τ = 1.15 ± 0.49 s (Figure 5, B and C). Depletion of LimE-GFP is slightly slower with an onset time of τ = 1.68 ± 0.43 s. These two sensors translocate to the boundary of the cell because Ras-GTP levels and F-actin levels increase, which must imply that there is a small time delay between the increase of Ras-GTP or F-actin and the depletion of the sensors from the cytoplasm. Calculations using fast but realistic binding kinetics of these sensors suggest that the delay may be between 0.5 and 1.5 s (see Supplemental Figure S1). Assuming a time delay of 0.75 s between the increase of Ras-GTP/F-actin and the depletion of the sensors, we deduce the following onset times in seconds after cAMP stimulation: Ras at 0.4 ± 0.5 s, sGC activation at 0.8 ± 0.4 s, cGMP increase at 0.8 ± 0.3 s, and F-actin at 0.9 ± 0.4 s, which are all fast and statistically not significantly different ($P > 0.1$); however, sGC-GFP translocation at 3.4 ± 0.5 s is significantly slower at $P < 0.01$.

Possible function of sGC-GFP association to the cytoskeleton. The function of the association of sGC to the branched F-actin in pseudopods and parallel F-actin in the contractile cortex was investigated in buffer and after stimulation with uniform cAMP, using the F-actin inhibitor LatA and the truncated protein ΔN-sGC that does not bind to the cytoskeleton (Veltman and Van Haastert, 2006; van Haastert, 2021). In buffer, sGC-GFP is mainly associated to branched F-actin in pseudopods and is nearly absent in the contractile cortex (see Figure 4A). Therefore, the effects of LatA or ΔN-sGC on cGMP levels in buffer may uncover the role of sGC association to the branched F-actin of pseudopods and not so much the role of the contractile cortex. Addition of LatA to wild-type cells or expression of ΔN-sGC in *gc*-null cells leads to a 40% decrease of basal cGMP levels of cells in buffer (Figure 6A). This suggests that interaction of sGC with the branched cytoskeleton may lead to increased cGMP synthesis, probably because pseudopod-associated sGC exhibits increased Mg^{2+}-dependent guanylyl cyclase activity.

cAMP does not induce an increase of sGC-GFP localization in pseudopods but a strong increase of sGC-GFP in the contractile cortex (Figure 4, B and C). This translocation of sGC-GFP does not occur in LatA and is also absent in *gc*-null cells expressing ΔN-sGC-GFP (Figure 4A). In these cells, with lower basal cGMP levels, cAMP induces a strong cGMP response that reaches higher maximal levels. Furthermore, these maximal levels are reached later and cGMP declines more slowly than in control cells; half-maximal recovery occurs at 20 s in wild type, at 30 s in ΔN-sGC, and at 50 s in LatA (Figure 6B). In wild-type cells cAMP-induced association of sGC to the cortex starts at 3.3 s after stimulation, at which time the enzyme is already fully activated. The cGMP response in LatA or *gc*-null cells expressing ΔN-sGC-GFP starts to become larger than the cGMP response of control wild-type cells beyond 5 s after stimulation, thus at the moment sGC-GFP in control cells associates to the cytoskeleton. This suggests that the association of sGC-GFP to the cortex actually inhibits sGC activity.

Regulation of sGC by GbpC, membrane interaction, and Ca^{2+}

Membrane interaction. In cells, sGC-GFP protein as detected by confocal microscopy is localized for about 80% in the cytosol and 20% at the boundary of the cell at or near the plasma membrane (Veltman *et al.*, 2005). The sGC activity measured with the substrate Mn^{2+}-GTP is also present mainly in the soluble fraction of the lysate (Table 3), confirming the general notion that Mn^{2+} uncovers intrinsic cyclase activity (Tesmer *et al.*, 1999; Roelofs *et al.*, 2001b). In contrast, guanylyl cyclase activity measured with the physiologically more relevant Mg^{2+}-GTP is detectable predominantly in the pellet fraction (Table 3). The pellet fraction may contain membranes, organelles, and cytoskeleton. In conclusion, it is unclear whether sGC in the pellet of a cell lysate or at the boundary of the cell in vivo is

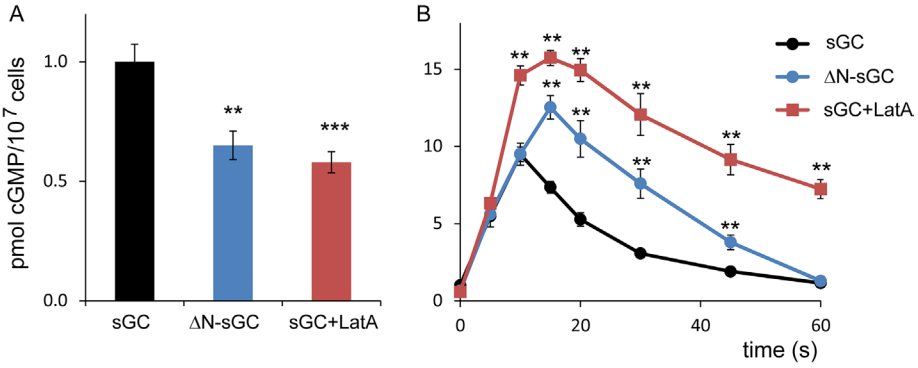

FIGURE 6: Potential role of sGC association to the cytoskeleton. (A) Basal cGMP levels in buffer. The interaction between sGC and F-actin is mainly to branched F-actin in pseudopods, which is absent in LatA and in ΔN-sGC, which both show reduced cGMP levels. (B) cAMP-stimulated cGMP levels. During cAMP stimulation the interaction between sGC and F-actin is mainly to parallel F-actin in the cortex, which is absent in LatA and in ΔN-sGC, which both show increased cGMP levels. The data shown are the means and SEM of six determinations; significantly different from wild type at **, $P < 0.01$ or ***, $P < 0.001$.

associated to the plasma membrane or to the F-actin cortex. Therefore, cells were incubated with 7.5 μM LatA for 15 min to deplete the cells of F-actin. In vivo all sGC-GFP becomes cytosolic (Veltman and Van Haastert, 2006; Figure 4A). Interestingly, the distribution of Mn^{2+}-GTP– and Mg^{2+}-GTP–dependent guanylyl cyclase activity in the supernatant and pellet fraction of LatA-treated cells is similar to the distribution between pellet and supernatant in a lysate from control cells (Table 3). Furthermore, similar results were obtained with ΔN-sGC-GFP expressed in *gc*-null cells: In cells ΔN-sGC-GFP does not bind to the F-actin cytoskeleton of the cortex (Figure 4A), but in lysates ΔN-sGC-GFP protein and Mn^{2+}-GTP activity are localized in the pellet and supernatant fraction as for the wild-type protein (Table 3). In addition, sGC from LatA-treated cells or ΔN-sGC-GFP is still activated by GTPγS in the pellet fractions (Table 3). This suggests that sGC localization in the pellet fraction is probably due to interaction with the membrane, not to association with the cytoskeleton.

The association of sGC to the membrane was analyzed in reconstitution experiments using membranes from *gc*-null cells (that do not contain sGC) with the supernatant of wild-type cells (that do contain sGC and Mn^{2+}-GTP activity, but no Mg^{2+}-GTP activity) (Veltman *et al.*, 2005). The results (Figure 7) show that incubation of the supernatant of wild-type cells with the pellet of *gc*-null cells leads to the appearance of Mg^{2+}-GTP–dependent guanylyl cyclase activity. Interestingly, the Mg^{2+}-GTP–dependent activity in the mixture is activated by GTPγS, while GTPγS has no effect on separate fractions. In addition, upon centrifugation this Mg^{2+}-GTP–dependent guanylyl cyclase activity is found largely in the pellet fraction, indicating that sGC from the supernatant of wild-type cells translocated to the pellet fraction of *gc*-null cells (Veltman *et al.*, 2005). Very similar results were obtained when mixing the supernatant of ΔN-sGC-GFP expressed in *gc*-null with the pellet of *gc*-null cells: low activity in the separate fractions and high activity in the mixture that is activated by GTPγS, indicating that ΔN-sGC-GFP can associate with the membrane binding sites to generate Mg^{2+}-GTP–dependent guanylyl cyclase activity that can now be stimulated by GTPγS.

By mixing different amounts of supernatant and pellet, it was deduced that the binding sites saturate with Mg^{2+}-GTP activity at a 1:1 ratio of supernatant and pellet (Veltman *et al.*, 2005). At this 1:1 mixture, we estimate that approximately 20% of the sGC molecules from the supernatant have associated with the pellet fraction (estimate based on Mn^{2+}-GTP activities in the original wild-type supernatant and in the pellet obtained after centrifugation of the mixture), suggesting that a cell contains about fivefold more sGC molecules than membrane binding sites for sGC. The formation of Mg^{2+}-GTP activity in these reconstitutions is not enhanced by GTPγS (Veltman *et al.*, 2005).

Regulation by Ca^{2+} ions. Micromolar concentrations of Ca^{2+} strongly inhibit sGC activity (Janssens *et al.*, 1989; Roelofs and Van Haastert, 2002): Lysis in the presence of 10 μM Ca^{2+} leads to full inhibition of GC activity (experiment 2 in Table 4). This inhibition is reversible, because the addition of EGTA to reduce free Ca^{2+} to <1 nM leads to the recovery of sGC activity and its activation by GTPγS (experiment 3). In a series of centrifugation and reconstitution experiments, the mechanism of how Ca^{2+} may inhibit sGC was investigated (Veltman *et al.*, 2005). In experiment 3, lysis of cells in

		sGC activity (pmol/min per equivalent of 10^7 cells)		
Enzyme	**Substrate**	**Pellet**	**Supernatant**	**% in pellet**
sGC	Mn^{2+}-GTP	12.6 ± 3.5 (8)	30.9 ± 4.4 (8)	29 ± 9
	Mg^{2+}-GTP	24.9 ± 3.4 (9)	4.5 ± 0.4 (9)	85 ± 13
	Mg^{2+}-GTP + GTPγS	50.1 ± 3.9 (9)	4.2 ± 0.7 (9)	
sGC in LatA	Mn^{2+}-GTP	12.0 ± 5.2 (8)	30.7 ± 7.5 (8)	28 ± 14
	Mg^{2+}-GTP	17.6 ± 4.8 (6)	2.6 ± 0.5 (6)	87 ± 28
	Mg^{2+}-GTP + GTPγS	37.2 ± 4.6 (6)	2.7 ± 0.8 (6)	
ΔN-sGC	Mn^{2+}-GTP	8.9 ± 4.9 (9)	28.6 ± 4.2 (9)	24 ± 5
	Mg^{2+}-GTP	18.5 ± 3.5 (8)	2.8 ± 0.3 (8)	87 ± 19
	Mg^{2+}-GTP + GTPγS	36.4 ± 1.4 (8)	3.1 ± 0.6 (8)	

Data are means and SD with *n* the number of determinations in parentheses.

TABLE 3: Membrane association and activity of sGC.

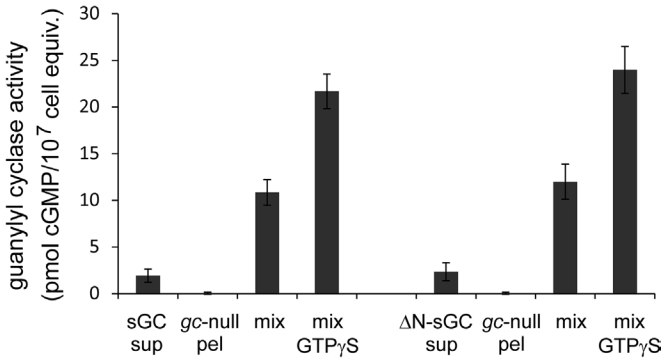

FIGURE 7: Reconstitution of sGC and ΔN-sGC with membranes. The supernatant of a lysate of sGC or ΔN-sGC cells was reconstituted with the pellet of *gc*-null cells and assayed with Mg^{2+}-GTP in the absence or presence of 50 μM GTPγS. The mixture has increased activity, which is further increased by GTPγS. Data shown are the means and SEM of five experiments with triplicate reconstitutions ($n = 15$).

Ca^{2+} and the addition of EGTA to the lysate, followed by centrifugation, lead to recovery of sGC activity in the pellet. This indicates that in EGTA sGC remained associated with the membrane binding sites. In experiment 4, cells were also lysed in Ca^{2+}, but EGTA was now added after centrifugation; the data show that no sGC was recovered in the pellet or supernatant. This indicates that in Ca^{2+}, sGC has dissociated from the membrane binding sites. Finally in experiment 5, this pellet prepared in Ca^{2+} was reconstituted with a fresh supernatant prepared in EGTA, leading to the recovery of sGC activity and its activation by GTPγS. This indicates that the sGC-binding sites in the membrane were not lost by centrifugation in Ca^{2+} and can still bind sGC in EGTA. Together the experiments suggest that 1) sGC binds to membrane binding sites, which supports Mg^{2+}-GTP–dependent guanylyl cyclase activity and activation by GTPγS; 2) in the presence of Ca^{2+}, sGC dissociates from these membrane binding sites and loses Mg^{2+}-GTP–dependent activity and activation by GTPgS, but the binding sites remain present in the membrane; 3) upon removal of Ca^{2+}, sGC can reassociate to the membrane binding sites and become active with Mg^{2+}-GTP and activated by GTPγS.

The role of Ca^{2+} in vivo was investigated for the cAMP-stimulated cGMP response in cells that were permeabilized by electroshock (Valkema and Van Haastert, 1992, 1994; Schoen *et al.*, 1996). The conditions used generate small holes that allow the transport of molecules smaller than about 300 Da. ATP and GTP do not pass, but ions such as Ca^{2+} can equilibrate with the external medium (Van Haastert *et al.*, 1989). Electroporation in the presence of 1 μM extracellular free Ca^{2+} using a EGTA/Ca^{2+} buffer leads to the rapid decline of basal cGMP levels with a half-time of about 30 s (Figure 8A). The cAMP-induced cGMP response of permeabilized cells in EGTA is larger than the cGMP response of control cells, whereas the cGMP response is strongly inhibited in buffered 1 μM and 1 mM extracellular Ca^{2+} (Figure 8B). Furthermore, the decline of cAMP-stimulated cGMP levels to basal levels between 10 and 45 s after stimulation shows a half-time of about 10 s for control cells and cells in EGTA and a half-time of about 6 s for permeabilized cells in 1 μM and 1 mM extracellular Ca^{2+} (Figure 8B). The experiments reveal that elevated concentrations of intracellular Ca^{2+} inhibit basal and cAMP-stimulated sGC activity. The extent and timing of the observed inhibition are similar to those of the expected inhibition that was predicted using a model that includes the biochemical properties of sGC and the cAMP-mediated increase of cellular Ca^{2+} (Valkema and Van Haastert, 1994).

Regulation of sGC by GbpC. The cGMP produced by sGC binds to GbpC, a large 294 kDa protein with multiple domains including a kinase domain (Bosgraaf *et al.*, 2002a; Kortholt *et al.*, 2012). Previously we have shown that a partially purified cGMP-binding activity regulates guanylyl cyclase activity in lysates of starved cells (Kuwayama and Van Haastert, 1996). Now we know that GbpC is the only high-affinity cGMP-binding protein of *Dictyostelium* (Van Egmond, 2010) and essentially all guanylyl cyclase activity of starved cells is attributed to sGC (Roelofs and Van Haastert, 2002). Therefore, these experiments are interpreted in the context of the regulation of cGMP-synthesizing enzyme sGC by the cGMP-target GbpC. With this interpretation, the results of Kuwayama and Van Haastert (1996) indicate that in vitro GbpC activates sGC to about 150% of control values when its kinase activity is inhibited by AppNHp; this activation is independent of the presence of cGMP. In contrast, in the presence of ATP, which allows kinase activity, GbpC inhibits sGC

No	Experiment	GTPγS	Activity (pmol/min per equivalent of 10^7 cells)		
			Lysate	Pellet	Supernatant
1	Lysis in EGTA, centrifugation, assay in EGTA	–	12.31 ± 4.53	12.77 ± 3.77	1.00 ± 0.49
		+	32.31 ± 4.14	41.01 ± 8.57	1.12 ± 0.51
2	Lysis in Ca^{2+}, centrifugation, assays in Ca^{2+}	–	1.38 ± 0.37	1.31 ± 0.56	0.43 ± 0.39
		+	0.92 ± 0.34	1.72 ± 0.39	0.44 ± 0.95
3	Lysis in Ca^{2+}, EGTA added, centrifugation, assay in EGTA	–	12.46 ± 5.27	11.54 ± 5.66	0.93 ± 0.27
		+	24.96 ± 5.93	27.23 ± 2.16	1.12 ± 0.27
4	Lysis in Ca^{2+}, centrifugation, assay in EGTA	–		1.92 ± 0.93	1.19 ± 0.56
		+		2.41 ± 1.10	1.11 ± 0.51
5	Reconstitution pellet 4 with supernatant 1, assay in EGTA	–		9.98 ± 1.79	
		+		18.81 ± 2.16	

Cells were lysed at 4°C in either 1.5 mM EGTA or 10 μM added Ca^{2+}; the lysate was centrifuged at 4°C for 1 min at 14,000 × *g*. Guanylyl cyclase activity was measured at 22°C in the lysate, the supernatant fraction, or the pellet fraction with Mg^{2+}-GTP in the absence or presence of 50 μM GTPγS. Data shown are the means and SD of two independent experiments in triplicate ($n = 6$). Experiment 5 is the reconstitution of the pellet of experiment 4 with the supernatant of experiment 1 (all indicated in yellow).

TABLE 4. Regulation of sGC–membrane interaction by Ca^{2+}.

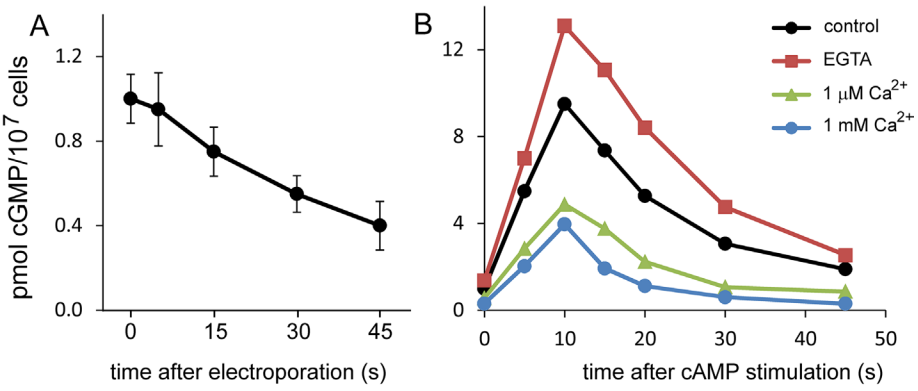

FIGURE 8: Regulation of sGC by Ca^{2+}. Cells were permeabilized by electroporation and incubated in Ca^{2+}/EGTA buffers. (A) Basal cGMP levels in 1 μM free Ca^{2+}; cells were electroporated at $t = 0$ s, and samples were taken at the times indicated (mean and SEM, $n = 4$). The sample at $t = 0$ was taken just before electroporation. (B) Cells were electroporated and incubated for 45 s at the indicated Ca^{2+} concentrations. Then the cells were stimulated at $t = 0$ s with 100 nM cAMP; control is the cGMP response of nonpermeabilized cells. Data are the means of two experiments with duplicate determinations.

activity to 60%; this inhibition is potentiated in the presence of cGMP to 36% of the control activity. Furthermore in the chemotaxis mutant KI-7, binding of cGMP to GbpC has altered affinity (Kuwayama *et al.*, 1995), and the cGMP/ATP-mediated inhibition of guanylyl cyclase is completely lost (Kuwayama and Van Haastert, 1996).

To address the regulation of sGC by GbpC in vivo, cGMP responses in relevant mutants (Kuwayama *et al.*, 1993; Bosgraaf *et al.*, 2002a) were analyzed. Basal cGMP levels of *gbpC*-null and KI-7 cells are not significantly different from that of their wild-type parental cells (Figure 9A). In contrast, the cAMP-induced cGMP responses in *gbpC*-null and KI-7 cells are elevated, with higher cGMP levels that reach maximal levels and recover basal cGMP levels later than in the wild-type parental cells; half-maximal recovery is 20 s in wild-type and 30–40 s in *gbpC*-null and KI-7 cells. The prolonged cGMP response of *gbpC*-null cells in vivo is consistent with the in vitro inhibition of sGC by cGMP-occupied GbpC.

DISCUSSION

The major guanylyl cyclase of starved *Dictyostelium* cells, sGC, is a largely soluble enzyme that is also associated to the F-actin cytoskeleton and that is activated by G-proteins at the plasma membrane. Here we dissect how the enzyme is activated and resolve the functions of localization in the F-actin cytoskeleton and at the plasma membrane (Figure 10).

Activation of sGC by cAMP does not require its association with the cytoskeleton

Two pieces of evidence reveal that the association of sGC to the branched or parallel F-actin is not required for its activation by cAMP in vivo or by GTPγS in vitro. First, the association of sGC with the F-actin cortex is relatively slow, with an onset time of about 3 s after stimulation. At that time moment, sGC is already fully activated (Figure 5). Second, depletion of the F-actin cytoskeleton with LatA or deletion of the N-terminus of sGC both inhibit translocation of sGC-GFP to the cortex but do not inhibit activation of the enzyme by cAMP (Figure 6).

In cell lysates sGC is present in both the pellet and the supernatant fraction, but only the enzyme in the pellet fraction is active with the physiologically relevant substrate Mg^{2+}-GTP and can then be activated by GTPγS. In lysates prepared from LatA-treated cells, the distribution of sGC protein between the pellet and soluble fraction is the same as in control cells, indicating that sGC in the pellet is attached to membrane, not to F-actin. Also ΔN-sGC, which does not bind to F-actin, still has a normal distribution between the pellet and supernatant (Table 3). Importantly, in the pellet fraction both sGC in LatA and ΔN-sGC are activated strongly by GTPγS, indicating that these enzymes not only interact normally with membranes but are also activated by the target of GTPγS that appears to be RasC/G (see below). The interaction of sGC with the cytoskeleton therefore does not play a role in its activation either in vivo by cAMP or by GTPγS in vitro.

Activation pathway of sGC by cAMP

The activation of sGC in mutants reveals a signaling pathway by cAMP in vivo that consists of cAR1, Gα2βγ, and RasC/G (Figure 1). Reconstitution of sGC with purified proteins in vitro shows that sGC is activated by GTP-bound active RasG, but not by inactive RasG-GDP, Gα, or Gβγ (Figure 3). This means that the acceptor protein for GTPγS-mediated activation of sGC in membranes is not a heterotrimeric G-protein but the monomeric RasC and RasG. Interestingly, activation of RasC/G is not sufficient for activation of sGC. This conclusion comes from two types of experiments. First, induced expression of dominant active RasG-G12V does not lead to an increase of basal or cAMP-stimulated cGMP levels. Second, experiments with cAMP stimulation of *gα2*-null cells and folate stimulation of *gα4*-null cells show a significant activation of Ras and F-actin formation, but no cGMP formation. In *gβ*-null cells, neither cAMP nor folate induces any of these responses (Table 2). This

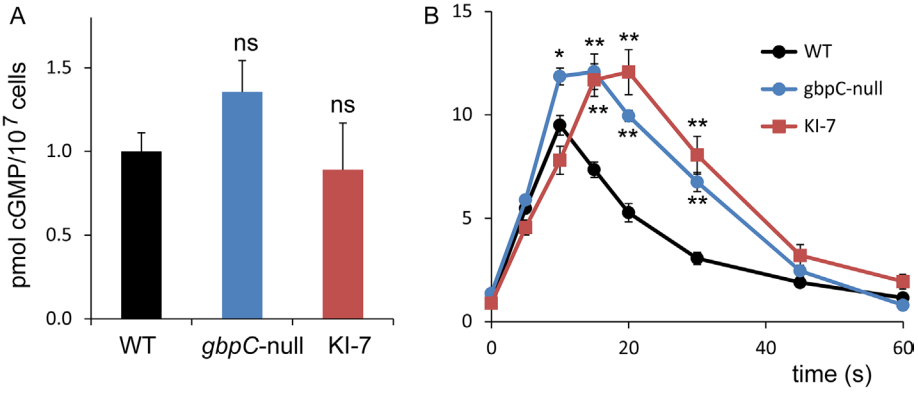

FIGURE 9: Regulation of sGC by its target protein GbpC. (A) Basal cGMP levels in buffer. (B) cAMP-stimulated cGMP levels. Mutant KI-7 has a defect in the regulation of sGC by GbpC (Kuwayama and Van Haastert, 1996). The data shown are the means and SEM of six determinations; significantly different from wild type at *, $P < 0.05$ or ***, $P < 0.01$; ns, not significant.

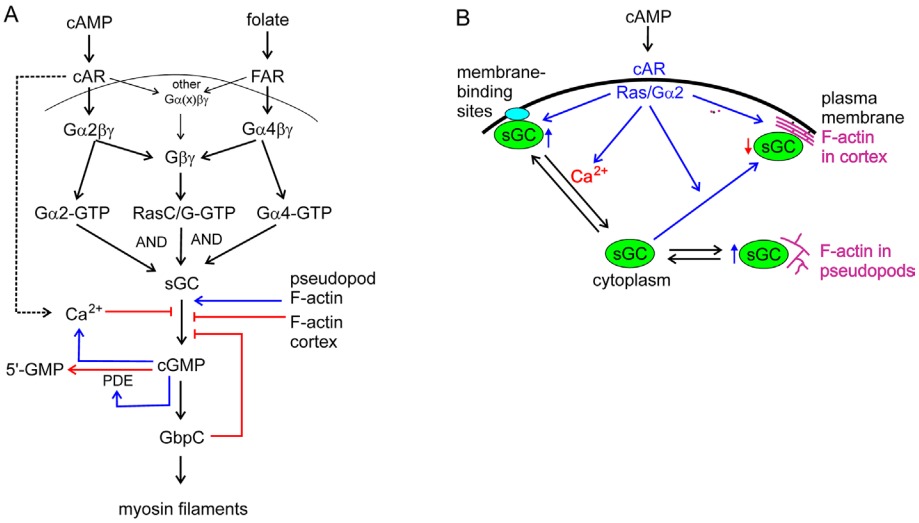

FIGURE 10: Model of the regulation of the cGMP pathway. (A) cGMP signaling pathway. Activation of cGC by cAMP in starved cells requires Gα2 *and* RasC/G, and activation by folate in vegetative cells requires Gα4 *and* RasC/G. The produced cGMP activates the cGMP-binding protein GbpC that induces myosin filament formation in the rear of the cell. The activity of sGC is regulated by multiple processes: inhibition by cAMP-stimulated and cGMP-potentiated Ca^{2+} increase, inhibition by parallel F-actin in the cortex, stimulation by branched F-actin in pseudopods and cGMP is degraded by a cGMP-stimulated phosphodiesterase. (B) Localization of sGC. Confocal images reveal that sGC-GFP is localized predominantly in the cytoplasm. sGC-GFP is enriched in pseudopods and at the cell boundary of the cell that is composed of the plasma membrane and the F-actin cortex. cGMP and guanylyl cyclase assays reveal that sGC in the cytoplasm is in equilibrium with association to branched F-actin in pseudopods and with association to the plasma membrane. sGC can also bind to parallel F-actin in the cortex that is formed upon cAMP stimulation. sGC associated to branched F-actin in pseudopods has increased activity. sGC associated to the membrane can be activated by Ras/Gα2; Ca^{2+} ions induce the dissociation of sGC from the membrane and thereby its inhibition. sGC associated to parallel F-actin in the cortex has reduced activity.

suggests that in vivo Ras is activated by Gβγ; in wild-type cells this is predominantly liberated from Gα2βγ by cAMP and from Gα4βγ by folate. In *gα2*-null cells, Gβγ can be liberated by cAMP from Gα1βγ or Gα9βγ; and in *gα4*-null cells, Gβγ can be liberated by folate from Gα5βγ (Figure 10). Therefore, we conclude that the activation of sGC by chemoattractants requires both Ras and Gα2 for cAMP, or Ras and Gα4 for folate. The requirement for the activation of Gβγ, Ras, and Gα2/Gα4 for the induction of a cGMP responses is also observed for TorC2 activation, PI3K activation, and chemotaxis (Kesbeke *et al.*, 1988; Liao *et al.*, 2013).

In lysates sGC in the soluble fraction can translocate to the pellet of *gc*-null cells and become activated by GTPγS (Figure 7). These membrane binding sites are half-maximally saturated at 20-fold-diluted lysates (compared with intact cells), and saturation occurs at equal amounts of pellet and cytosol fraction (on a cell lysate basis). Approximately 25% of sGC protein is found in the pellet fraction, suggesting that the number of binding sites is only one-fourth the number of sGC molecules. These data also suggest that in cells, in which the protein concentration is much higher than in a lysate, all binding sites are occupied with sGC. The nature of these sGC-binding sites in the membrane is currently unknown. Ca^{2+} inhibits binding of sGC to the membrane, which is reversible. Binding of sGC to the membrane is required for its activation by GTPγS, because GTPγS does not activate sGC in the presence of Ca^{2+} (Table 4). Furthermore, cells with holes made by electroporation exhibit a very good cAMP-induced cGMP response in EGTA but not in the presence of 1 μM free Ca^{2+} (Figure 8). cAMP induces the rapid rise of intracellular Ca^{2+} concentration from about 50 to 200 nM (Abe *et al.*, 1988). This Ca^{2+} comes from uptake and from release of intracellular Ca^{2+} stores (Europe-Finner and Newell, 1986; Milne and Coukell, 1991) and is enhanced by cGMP (Kuwayama and Van Haastert, 1998a). The combined results suggest a model in which sGC reversibly binds to a limited number of membrane binding sites in a Ca^{2+}-dependent manner. This membrane binding of sGC is essential for Mg^{2+}-GTP–dependent activity, for stimulation by GTPγS/Ras in vitro and by cAMP in vivo. The cAMP-mediated increase of Ca^{2+} induces the dissociation of sGC from the membrane, leading to a loss of Mg^{2+}-GTP–dependent guanylyl cyclase activity. The detection of sGC-GFP in membranes of live cells is complicated for several reasons. First, sGC-GFP is about twofold overexpressed (Veltman *et al.*, 2005), while the binding sites are very limited (20% of endogenously expressed sGC), suggesting that only ~10% of sGC-GFP can be found at the membrane. Second, in cells sGC-GFP is also associated with the cortex, which spatially cannot be distinguished from the plasma membrane in confocal images. cAMP is shown to induce a 20–30% increase of sGC-GFP association to the cortex, while at the same time cAMP is expected to induce a Ca^{2+}-mediated dissociation of sGC-GFP from the membrane. We have reinvestigated the potential association–dissociation of sGC-GFP to the membrane in specifically designed experiments to have maximal relative binding to the membrane; these experiments include relatively low expression of ΔN-sGC-GFP that does not bind to the cortex or LatA-treated cells expressing sGC-GFP and cytosolic RFP to obtain a very sensitive assay for the localization of membrane-associated proteins (Bosgraaf *et al.*, 2008). At these conditions, we observed that maximally 3% of ΔN-sGC-GFP or sGC-GFP is present at the boundary of the cell, which is at the limit of sensitivity of the experiment (Bosgraaf *et al.*, 2008). We conclude that in vivo less sGC-GFP is associated with the membrane than expected from the in vitro experiments.

Association of sGC to the cytoskeleton inhibits the enzyme

The association of sGC to the cortex starts relatively late at about 3 s after cAMP stimulation and lasts long (half decline at about 20 s). In LatA or with ΔN-sGC, the cGMP response starts as in control cells but reaches a larger maximum that is obtained later, and cGMP levels decline much slower than in control cells. This suggests that the association of sGC to the cytoskeleton actually inhibits enzyme activity. This inhibition contributes to the multiple feedback mechanisms responsible for the rapid decline of cGMP to basal levels. These mechanisms include the above-mentioned Ca^{2+}-mediated inhibition of sGC, the stimulation of a cGMP phosphodiesterase by cGMP (Van Haastert *et al.*, 1982a), and inhibition of sGC by the cGMP-target GbpC (see below).

Regulation of sGC activity and localization by its target GbpC

Mutant *gbpC*-null cells exhibit an increased and prolonged cGMP response. This observation is compatible with the in vitro observation that GbpC, in a cGMP- and ATP-dependent manner, inhibits sGC activity. This would lead to a delayed negative feedback loop of inhibition of further cGMP synthesis by the cGMP-stimulated target. No evidence is available for other potential explanations of the prolonged response in *gbpC*-null cells; no evidence for altered cGMP-PDE activity in *gbpC*-null cells (Bosgraaf *et al.*, 2002a) and no evidence for decreased association of sGC to the cortex in *gbpC*-null cells (that would lead to decreased inhibition). Actually, sGC-GFP appears to be stronger associated to the cortex in *gbpC*-null cells in buffer and upon cAMP stimulation (Tanabe *et al.*, 2018).

Function and regulation of sGC in buffer

In cells in buffer, sGC is present predominantly in the cytosol, and partly in the membrane and in the branched F-actin in pseudopods. Patches of activated Ras induce branched F-actin and new pseudopods. Although sGC in the membrane is activated by Ras in vitro, this probably does not occur in vivo because sGC activation requires the costimulation by a Gα protein that is likely not to be activated in the absence of cAMP. Conversely, sGC in the branched F-actin is likely to have enhanced activity, because inhibition of the cytoskeletal localization of sGC, either by LatA or in ΔN-sGC, leads to a 40% reduction of basal cGMP levels. This would suggest that strong pseudopod activity in the front of the cell would lead to enhanced cGMP levels (Van Haastert, 2020). cGMP mediates myosin II–filament formation in the rear of the cell, leading to a front-to-rear polarization of that cell (Bosgraaf and van Haastert, 2006). New pseudopods are suppressed in the rear by which they preferentially are formed in the current front of the cell. As a consequence, cells tend to continue movement in the same direction. This persistence enhances the dispersion of cells over larger distances for optimal food searching.

Function and regulation of sGC in a shallow gradient of cAMP

Cells in a shallow cAMP gradient can be regarded as cells in buffer with a weak activation of cAMP receptors that is slightly stronger in the front than in the rear of the cell. For sGC regulation the description above for buffer still holds but with one important addition: cAMP induces the activation of Gα2βγ in an intracellular gradient that is proportional to the gradient of cAMP (Janetopoulos *et al.*, 2001). Therefore, the activated Gα2-GTP in the front of the cell can now synergize with Ras-GTP patches to activate sGC. Thus in a shallow cAMP gradient, sGC is still activated in the branched F-actin of pseudopods and is activated additionally in the membrane in Ras-GTP patches. This likely will lead to a stronger cGMP response in the front of the cell than in buffer and therefore in a stronger cell polarity.

Function and regulation of sGC in cAMP oscillations

In buffer and in a shallow stable cAMP gradient, regulation of sGC by feedback loops such as Ca^{2+}, GbpC, and PDE5 is probably not very pronounced, because sGC is only weakly activated leading to a small but persistent increase of basal cGMP levels. In contrast, during cAMP oscillations sGC becomes fully activated as well as the other signaling pathways, leading to the full spectrum of regulatory processes. The activation of sGC by Ras/Gα2 occurs within 1 s of cAMP addition (Figure 5). Subsequently, sGC translocates to the cAMP-induced F-actin in the cortex, leading to reduced sGC activity. In addition, cAMP induces an increase of intracellular Ca^{2+} that inhibits sGC activation through dissociation of sGC from the membrane. Intracellular cGMP enhances the Ca^{2+} response. Furthermore, the produced cGMP binds to GbpC, leading to the further reduction of sGC activity. Finally, the produced cGMP activates the cGMP-PDE, leading to the fast degradation of cGMP levels. These combined activities during the rising phase of a cAMP oscillation lead to a short burst of cGMP, which leads to the complete disassembly of myosin II in the cortex (Bosgraaf and van Haastert, 2006). The cell cringes and loses all polarity (Futrelle *et al.*, 1982; Varnum and Soll, 1984; Berlot *et al.*, 1985). Then the cell recovers by extending a new pseudopod that is induced by a patch of activated Ras-GTP at the side of the cell exposed to the highest cAMP concentration (Sasaki *et al.*, 2004; Xiong *et al.*, 2010; Kortholt *et al.*, 2013). While the cell extends a new pseudopod, myosin II filaments are formed in the cortex at the rear of the cell providing a new polarity axis of the cell.

Function of the sGC protein sensu stricto

The above discussion describes the function of cGMP produced by sGC. However, the sGC protein itself supports chemotaxis, as was deduced from a point mutation in the catalytic domain mutant (Veltman and Van Haastert, 2006). This mutant sGC protein cannot produce cGMP, but otherwise is localized as the wild-type protein. Cells lacking guanylyl cyclases (*gc*-null cells) do not produce cGMP, have poor polarity with the extension of pseudeupods from the rear, and orient poorly in the direction of the cAMP gradient. *gc*-null cells expressing this catalytically inactive sGC mutant also have very poor polarity and extend pseudopods in the rear, but now the pseudopods in the front are much better oriented toward the cAMP gradient. This function of the sGC protein therefore does not require the catalytic domain, but absolutely requires the N-terminal part that is responsible for localization on the F-actin cytoskeleton. This function of sGC also requires the C-terminal AAA-ATPase domain (Veltman and Van Haastert, 2006).

Conclusions

The regulation of sGC during *Dictyostelium* cell movement and chemotaxis has multiple layers. The enzyme can be associated to the membrane where it is activated by Gα-GTP and Ras-GTP, which requires the activation of a GPCR by the chemoattactant cAMP or folate. The enzyme can also be associated with the branched F-actin in pseudopods where it has increased activity, or with the parallel F-actin in the cortex of the rear of the cell where it has reduced activity. sGC functions as enzyme producing cGMP that induces myosin II filaments in the cortex of the rear of the cell, thereby stabilizing the front-to-rear polarity axis. sGC also functions as a protein independent of its cyclase activity to regulate the formation of branched F-actin and pseudopods in the front of the cell. It is currently not known whether cGMP that is formed in the front of the cell has a role at its place of formation before it diffuses into the cell and regulates myosin in the rear of the cell. Similarly, it is unknown whether the sGC protein has a function in the cortex of the rear of the cell, beside inhibition of cyclase activity. Other open questions are how sGC interacts with the membrane, whether it is regulated by phosphorylation, or whether it is functional in a complex with other proteins.

MATERIALS AND METHODS

Request a protocol through *Bio-protocol*.

Cell lines and plasmids

The cell lines used are the strains mentioned in the text with references. In all cases the parental strain of the mutant was used as

control, as indicated in the figure legends. Strains *rasC*-null/RasG-S17N (Kortholt *et al.*, 2013) and RasG-G12V were made as follows: RasG-S17N was amplified by PCR, sequenced, and ligated into the *Bgl*II site of the previously characterized *Dictyostelium* extrachromosomal Tet-ON plasmids pDM310 (Veltman *et al.*, 2009b); the plasmid was transformed to a *rasC*-null strain (Bolourani *et al.*, 2006). RasG-G12V was amplified by PCR, sequenced, ligated into the Tet-ON plasmids pDM310 and transformed to AX3 cells.

Cells were grown in HL5-C media (Formedium, Norfolk, UK) either on Nunclon-coated Petri dishes or in shaking flasks. For selection, the medium was supplemented with the appropriate antibiotics; 10 µg/ml G418, 50 µg/ml hygromycine B, or 10 µg/ml blasticidine S. Induction of RasG-S17N or RasG-G12V was with 10 µg/ml doxycycline during the last 24 h of growth.

Cells were harvested, washed, and starved in 10 mM KH_2PO_4/Na_2HPO_4, pH 6.5 (PB). Generally, cells for biochemical experiments were starved in suspension by shaking in PB at a density of 10^7 cells/ml for 5 h. For microscopy, cells were starved on plates at a density of 2.5×10^5 cells/cm^2.

Protein purification

GST-RapA, GST-RasG, and GST-Gα4 were expressed in Rosetta DE3 cells (Novagen) from a pGEX4T1 plasmid containing an N-terminal GST and TEV cleavage side (Kataria *et al.*, 2013; Liu *et al.*, 2016). GST-Gβ and Gγ were coexpressed in *Dictyostelium* from a pDM314 plasmid (Veltman *et al.*, 2009a). Proteins were isolated by GSH affinity chromatography and cleaved with TEV protease (Kortholt *et al.*, 2006). The G-proteins were loaded with GppNHp or GDP by incubating them in the presence of 10 mM EDTA and a 20-fold excess of the nucleotide for 2 h at room temperature; the excess of nucleotide was removed by size exclusion chromatography (Kortholt *et al.*, 2006). The purified proteins were analyzed by SDS–PAGE, and the concentration was determined by Bradford's method (Bio-Rad).

cGMP formation

Cells were harvested, washed, and starved in suspension by shaking in PB at a density of 10^7 cells/ml for 5 h. After starvation, the cells were washed in PB, resuspended to a density of 1×10^8 cells/ml in PB, and aerated for at least 10 min. Cells were stimulated by adding 10 µl of cAMP solution to 40 µl of cell suspension, yielding a final concentration of 100 nM cAMP. The reaction was stopped at the indicated time points by adding 50 µl of 3.5% perchloric acid to the cell suspension. Samples were neutralized by adding 25 µl of 50% saturated $KHCO_3$ and incubated for 5 min at room temperature to allow the CO_2 to escape. After checking the correct pH, the samples were centrifuged for 5 min at 14,000 × *g* and the cGMP levels of the supernatant were determined by isotope dilution assays, using commercial kits (cGMP-[^{3}H] Biotrak Assay kit [Amersham] or a direct cGMP Enzyme Immunoassay Kit [Sigma-Aldrich]) or using a homemade kit with anti-cGMP antibody AB99 (Janssens *et al.*, 1989) as described in detail in Van Haastert (2006). Generally, triplicate time points were taken in each experiment and experiments were performed at least three times.

Guanylyl cyclase assay

Cells were harvested, washed and starved in suspension by shaking in PB at a density of 10^7 cells/ml for 5 h. Starved cells were washed and resuspended in 10 mM Tris, pH 8.0, to a density of 2×10^8 cells/ml. All subsequent steps were performed at 4°C and are described below for the standard procedure; deviations from this protocol are described in the legends to the figures and tables. One volume of cell suspension was mixed with one volume of lysis buffer, yielding 15 mM Tris, 250 mM sucrose, and 3 mM EGTA, pH 8.0, and the cells were lysed through a 3-µm Nuclepore polycarbonate membrane (Whatman). Guanylyl cyclase assays were performed at 22°C in a total volume of 150 µl with 75 µl of cell lysate and 75 µl of assay mixture, yielding final concentrations of 15 mM Tris, pH 8.0, 250 mM sucrose, 0.5 mM GTP, 10 mM 1,4-dithiothreithol, 1.5 mM EGTA, and 2.5 mM $MnCl_2$ or 2.5 mM $MgCl_2$ in the absence or presence of 50 µM GTPγS to activate G-proteins. Reactions were terminated after 20, 40, and 60 s by the addition of 40 µl of assay mixture to an equal volume of 3.5% perchloric acid. A 0 s time point was taken by adding 20 µl of lysate to a tube containing 40 µl of perchloric acid and 20 µl of assay buffer. Samples were neutralized by adding 20 µl of 50% saturated $KHCO_3$ and incubated for 5 min at room temperature to allow the CO_2 to escape. Samples were then centrifuged 5 min at 14,000 × *g*, and the cGMP levels of the supernatant were determined as described above. Activation by GTPγS in mutants (Figure 2) is expressed as the fold stimulation by GTPγS in the mutant relative to fold stimulation by the GTPγS parental strain, that is, (activity mutant with GTPγS/activity mutant without GTPγS –1)/(activity parental in GTPγS/activity parental without GTPγS –1).

For reconstitution experiments of guanylyl cyclase with purified proteins (Figure 3), starved AX3 cells were resuspended to a density of 4×10^8 cells/ml and lysed on ice. The lysate (25 µl) was incubated for 45 s on ice with 25 µl of lysis buffer, purified proteins, or GTPγS. Then tubes were transferred to 22°C, and 30 s later the guanylyl assay was started at 22°C by the addition of 50 µl of assay mixture. The final concentrations in the guanylyl cyclase assay were 15 mM Tris, pH 8.0, 250 mM sucrose, 0.5 mM GTP, 10 mM 1,4-dithiothreithol, 1.5 mM EGTA, 2.5 mM $MgCl_2$, and 5 µM activator proteins or 50 µM GTPγS. Reactions were terminated after 30 and 60 s by the addition of 40 µl of assay mixture to an equal volume of 3.5% perchloric acid. The 0 s time points were taken by adding 10 µl of lysate to a tube containing 40 µl of perphloric acid, 10 µl of activator protein, and 20 µl of assay buffer.

For reconstitution of sGC or ΔN-sGC with membranes (Figure 7), the following three cell lines were used: sGC expressed in *gc*-null, ΔN-sGC expressed in *gc*-null, and *gc*-null cells. Cells were starved and lysed following the standard procedure. The lysates were centrifuged at 4°C for 1 min at 14,000 × *g*. The experiment uses the supernatants of sGC and ΔN-sGC lysates and the pellet of *gc*-null lysate resuspended to the original volume in lysis buffer. The guanylyl cyclase assay was performed at 22°C in 15 mM Tris, pH 8.0, 250 mM sucrose, 0.5 mM GTP, 10 mM 1,4-dithiothreithol, 1.5 mM EGTA, and 2.5 mM $MgCl_2$ and contained in a total volume of 150 µl: 37.5 µl of supernatant from sGC or ΔN-sGC lysate and/or 37.5 µl of resuspended pellet from *gc*-null lysate and 50 µM GTPγS as indicated in the figure.

Microscopy

Cells were transformed with plasmids for the expression of sGC-GFP (Veltman and Van Haastert, 2006), ΔN-sGC-GFP (Veltman and Van Haastert, 2006), RBD-Raf-GFP/cytosolic RFP (Kortholt *et al.*, 2013), or LimE-GFP (Kortholt *et al.*, 2011). Cells were harvested, washed, and starved in PB on plates at a density of 2.5×10^5 cells/cm^2. For optimal development, *gα2*-null and *gβ*-null cells expressing GFP markers (Table 2) were mixed 1:1 with unmarked AX3 cells during starvation (Kortholt *et al.*, 2013). Starved cells were harvested and suspended in PB and used for microscopy recordings, using confocal laser scanning microscopy (Zeiss LSM800; 63× numerical aperture 1.4 objective). The images were recorded at a rate of 1 frame per second and an *x*,*y*-resolution of 63 or 198 nm.

Statistics and reuse of data

The data presented are often composed of the original data obtained from different published sources as indicated in the text, supplemented with unpublished experiments. Data of a mutant were always analyzed with its own parental stain. For instance, the data for *gα2*-null cells in Figure 1 are composed of mutant fgdA strain HC85 with parental XP55 (Kesbeke *et al.*, 1988), *gα2*-null strain JH104 with its parental JH130 (Kumagai *et al.*, 1991), the similar *gα2*-null strain MP2 with its parental HSP400 (Kuwayama and Van Haastert, 1998b), and the *gα2*-null strain DBS0236575 with its parental DH1 (Kumagai *et al.*, 1989) and supplemented with not previously published data on cGMP response using the *gα2*-null strains JH104 and DBS0236575. In a typical experiment the cGMP levels were measured in triplicate. The average response at $t = 10$ s after cAMP stimulation minus basal in the mutant is presented relative to the response in its parental strain. Reported are the means and SEM in figures and means and SD in tables (Cumming *et al.*, 2007). The number of independent observations (n) is the number of individual experiments, which for *gα2*-null cells ($n = 9$) is composed of three experiments with HC85, one experiment with JH104, three experiments with MP2, and two experiments with DBS0236575. The result for *gα2*-null cells is 1.7% ± 4.0% (mean and SD, $n = 9$) compared with the cGMP response of the parental strains.

Statistical significance was tested with the Student's t test; two tests were performed: comparison with the 100% response of the parental strain and comparison with 0% response. For the cGMP response of *gα2*-null cells, 1.7% ± 4.0% (mean and SD, $n = 9$) is highly significantly different from 100% at $P < 0.001$ but is not significantly different from 0% at $P > 0.1$.

ACKNOWLEDGMENTS

We thank all the lab members and funding agencies that have contributed to cGMP research during the past 45 years.

REFERENCES

Abe T, Maeda Y, Iijima T (1988). Transient increase of the intracellular Ca2+ concentration during chemotactic signal transduction in Dictyostelium discoideum cells. Differentiation 39, 90–96.

Bader S, Kortholt A, Van Haastert PJM (2007). Seven Dictyostelium discoideum phosphodiesterases degrade three pools of cAMP and cGMP. Biochem J 402, 153–161.

Berlot CH, Spudich JA, Devreotes PN (1985). Chemoattractant-elicited increases in myosin phosphorylation in Dictyostelium. Cell 43, 307–314.

Bolourani P, Spiegelman GB, Weeks G (2006). Delineation of the roles played by RasG and RasC in cAMP-dependent signal transduction during the early development of Dictyostelium discoideum. Mol Biol Cell 17, 4543–4550.

Bolourani P, Spiegelman G, Weeks G (2008). Rap1 activation in response to cAMP occurs downstream of ras activation during Dictyostelium aggregation. J Biol Chem 283, 10232–10240.

Bolourani P, Spiegelman G, Weeks G (2010). Ras proteins have multiple functions in vegetative cells of Dictyostelium. Eukaryot Cell 9, 1728–1733.

Bominaar AA, Van Haastert PJM (1994). Phospholipase C in Dictyostelium discoideum. Identification of stimulatory and inhibitory surface receptors and G-proteins. Biochem J 297(Pt 1), 189–193.

Bonner JT (1947). Evidence for the formation of cell aggregates by chemotaxis in the development of the slime mold Dictyostelium discoideum. J Exp Zool 106, 1–26.

Bosgraaf L, Keizer-Gunnink I, Van Haastert PJM (2008). PI3-kinase signaling contributes to orientation in shallow gradients and enhances speed in steep chemoattractant gradients. J Cell Sci 121, 3589–3597.

Bosgraaf L, Russcher H, Smith JL, Wessels D, Soll DR, Van Haastert PJM (2002a). A novel cGMP signalling pathway mediating myosin phosphorylation and chemotaxis in Dictyostelium. EMBO J 21, 4560–4570.

Bosgraaf L, Russcher H, Snippe H, Bader S, Wind J, Van Haastert PJM (2002b). Identification and characterization of two unusual cGMP-stimulated phoshodiesterases in dictyostelium. Mol Biol Cell 13, 3878–3889.

Bosgraaf L, Van Haastert PJM (2002). A model for cGMP signal transduction in Dictyostelium in perspective of 25 years of cGMP research. J Muscle Res Cell Motil 23, 781–791.

Bosgraaf L, van Haastert PJM (2006). The regulation of myosin II in Dictyostelium. Eur J Cell Biol 85, 969–979.

Bretschneider T, Siegert F, Weijer CJ (1995). Three-dimensional scroll waves of cAMP could direct cell movement and gene expression in Dictyostelium slugs. Proc Natl Acad Sci USA 92, 4387–4391.

Brzostowski JA, Johnson C, Kimmel AR (2002). Galpha-mediated inhibition of developmental signal response. Curr Biol 12, 1199–1208.

Chattwood A, Bolourani P, Weeks G (2014). RasG signaling is important for optimal folate chemotaxis in Dictyostelium. BMC Cell Biol 15, 13.

Cumming G, Fidler F, Vaux DL (2007). Error bars in experimental biology. J Cell Biol 177, 7–11.

Davidson AJ, Wood W (2016). Unravelling the actin cytoskeleton: a new competitive edge? Trends Cell Biol 26, 569–576.

de Wit RJ, Konijn TM (1983). Identification of the acrasin of Dictyostelium minutum as a derivative of folic acid. Cell Differ 12, 205–210.

De Wit RJ, van Bemmelen MX, Penning LC, Pinas JE, Calandra TD, Bonner JT (1988). Studies of cell-surface glorin receptors, glorin degradation, and glorin-induced cellular responses during development of Polysphondylium violaceum. Exp Cell Res 179, 332–343.

Dharmawardhane S, Cubitt AB, Clark AM, Firtel RA (1994). Regulatory role of the G alpha 1 s ubunit in controlling cellular morphogenesis in Dictyostelium. Development 120, 3549–3561.

Europe-Finner GN, Newell PC (1986). Inositol 1,4,5-triphosphate induces calcium release from a non-mitochondrial pool in amoebae of Dictyostelium. Biochim Biophys Acta 887, 335–340.

Futrelle RP, Traut J, McKee WG (1982). Cell behavior in Dictyostelium discoideum: preaggregation response to localized cyclic AMP pulses. J Cell Biol 92, 807–821.

Hadwiger JA (2007). Developmental morphology and chemotactic responses are dependent on G alpha subunit specificity in Dictyostelium. Dev Biol 312, 1–12.

Hadwiger JA, Lee S, Firtel RA (1994). The G alpha subunit G alpha 4 couples to pterin receptors and identifies a signaling pathway that is essential for multicellular development in Dictyostelium. Proc Natl Acad Sci USA 91, 10566–10570.

Janetopoulos C, Jin T, Devreotes P (2001). Receptor-mediated activation of heterotrimeric G-proteins in living cells. Science 291, 2408–2411.

Janssens PM, De Jong CC, Vink AA, Van Haastert PJM (1989). Regulatory properties of magnesium-dependent guanylate cyclase in Dictyostelium discoideum membranes. J Biol Chem 264, 4329–4335.

Kamp M (2019). Regulation of G-Protein during Chemotaxis in Space and Time. PhD Thesis. Groningen, the Netherlands: Groningen University.

Kataria R, Xu X, Fusetti F, Keizer-Gunnink I, Jin T, Van Haastert PJM, Kortholt A (2013). Dictyostelium Ric8 is a nonreceptor guanine exchange factor for heterotrimeric G proteins and is important for development and chemotaxis. Proc Natl Acad Sci USA 110, 6424–6429.

Kesbeke F, Snaar-Jagalska BE, Van Haastert PJM (1988). Signal transduction in Dictyostelium fgd A mutants with a defective interaction between surface cAMP receptors and a GTP-binding regulatory protein. J Cell Biol 107, 521–528.

Khosla M, Spiegelman GB, Insall R, Weeks G (2000). Functional overlap of the dictyostelium RasG, RasD and RasB proteins. J Cell Sci 113(Pt 8), 1427–1434.

Konijn TM (1969). Effect of bacteria on chemotaxis in the cellular slime molds. J Bacteriol 99, 503–509.

Konijn TM, Van De Meene JG, Bonner JT, Barkley DS (1967). The acrasin activity of adenosine-3′,5′-cyclic phosphate. Proc Natl Acad Sci USA 58, 1152–1154.

Kortholt A, Kataria R, Keizer-Gunnink I, Van Egmond WN, Khanna A, Van Haastert PJM (2011). Dictyostelium chemotaxis: essential Ras activation and accessory signalling pathways for amplification. EMBO Rep 12, 1273–1279.

Kortholt A, Keizer-Gunnink I, Kataria R, Van Haastert PJM (2013). Ras activation and symmetry breaking during Dictyostelium chemotaxis. J Cell Sci 126, 4502–4513.

Kortholt A, Rehmann H, Kae H, Bosgraaf L, Keizer-Gunnink I, Weeks G, Wittinghofer A, Van Haastert PJM (2006). Characterization of the GbpD-activated Rap1 pathway regulating adhesion and cell polarity in Dictyostelium discoideum. J Biol Chem 281, 23367–23376.

Kortholt A, Van Egmond WN, Plak K, Bosgraaf L, Keizer-Gunnink I, Van Haastert PJM (2012). Multiple regulatory mechanisms for the Dictyostelium Roco protein GbpC. J Biol Chem 287, 2749–2758.

Kumagai A, Hadwiger JA, Pupillo M, Firtel RA (1991). Molecular genetic analysis of two G alpha protein subunits in Dictyostelium. J Biol Chem 266, 1220–1228.
Kumagai A, Pupillo M, Gundersen R, Miake-Lye R, Devreotes PN, Firtel RA (1989). Regulation and function of G alpha protein subunits in Dictyostelium. Cell 57, 265–275.
Kuwayama H, Ishida S, Van Haastert PJM (1993). Non-chemotactic Dictyostelium discoideum mutants with altered cGMP signal transduction. J Cell Biol 123, 1453–1462.
Kuwayama H, Van Haastert PJ (1996). Regulation of guanylyl cyclase by a cGMP-binding protein during chemotaxis in Dictyostelium discoideum. J Biol Chem 271, 23718–23724.
Kuwayama H, Van Haastert PJM (1998a). cGMP potentiates receptor-stimulated $Ca2^{+}$ influx in Dictyostelium discoideum. Biochim Biophys Acta 1402, 102–108.
Kuwayama H, Van Haastert PJM (1998b). Chemotactic and osmotic signals share a cGMP transduction pathway in Dictyostelium discoideum. FEBS Lett 424, 248–252.
Kuwayama H, Viel GT, Ishida S, Van Haastert PJM (1995). Aberrant cGMP-binding activity in non-chemotactic Dictyostelium discoideum mutants. Biochim Biophys Acta 1268, 214–220.
Liao X-H, Buggey J, Lee YK, Kimmel AR (2013). Chemoattractant stimulation of TORC2 is regulated by receptor/G protein-targeted inhibitory mechanisms that function upstream and independently of an essential GEF/Ras activation pathway in Dictyostelium. Mol Biol Cell 24, 2146–2155.
Liu Y, Lacal J, Veltman DM, Fusetti F, van Haastert PJM, Firtel RA, Kortholt A (2016). A Gα-stimulated RapGEF is a receptor-proximal regulator of Dictyostelium chemotaxis. Dev Cell 37, 458–472.
Mato J, Konijn T (1977). Chemotactic signals and cyclic GMP accumulation in Dictyostelium. In: Development and Differentiation in the Cellular Slime Moulds, ed. C. Ashworth, Amsterdam: Elsevier/North-Holland Biomedical Press, 93–103.
Mato JM, Krens FA, Van Haastert PJM, Konijn TM (1977). 3′:5′-cyclic AMP-dependent 3′:5′-cyclic GMP accumulation in Dictyostelium discoideum. Proc Natl Acad Sci USA 74, 2348–2351.
Meima ME, Biondi RM, Schaap P (2002). Identification of a novel type of cGMP phosphodiesterase that is defective in the chemotactic stmF mutants. Mol Biol Cell 13, 3870–3877.
Milne JL, Coukell MB (1991). A Ca2+ transport system associated with the plasma membrane of Dictyostelium discoideum is activated by different chemoattractant receptors. J Cell Biol 112, 103–110.
Pan M, Neilson MP, Grunfeld AM, Cruz P, Wen X, Insall RH, Jin T (2018). A G-protein-coupled chemoattractant receptor recognizes lipopolysaccharide for bacterial phagocytosis. PLoS Biol 16, e2005754.
Pan M, Xu X, Chen Y, Jin T (2016). Identification of a chemoattractant G-protein-coupled receptor for folic acid that controls both chemotaxis and phagocytosis. Dev Cell 36, 428–439.
Pan P, Hall EM, Bonner JT (1972). Folic acid as second chemotactic substance in the cellular slime moulds. Nat New Biol 237, 181–182.
Roelofs J, Loovers HM, Van Haastert PJM (2001a). GTPgammaS regulation of a 12-transmembrane guanylyl cyclase is retained after mutation to an adenylyl cyclase. J Biol Chem 276, 40740–40745.
Roelofs J, Meima M, Schaap P, Van Haastert PJM (2001b). The Dictyostelium homologue of mammalian soluble adenylyl cyclase encodes a guanylyl cyclase. EMBO J 20, 4341–4348.
Roelofs J, Snippe H, Kleineidam RG, Van Haastert PJM (2001c). Guanylate cyclase in Dictyostelium discoideum with the topology of mammalian adenylate cyclase. Biochem J 354, 697–706.
Roelofs J, Van Haastert PJM (2002). Characterization of two unusual guanylyl cyclases from dictyostelium. J Biol Chem 277, 9167–9174.
Rottner K, Faix J, Bogdan S, Linder S, Kerkhoff E (2017). Actin assembly mechanisms at a glance. J Cell Sci 130, 3427–3435.
Sasaki AT, Chun C, Takeda K, Firtel RA (2004). Localized Ras signaling at the leading edge regulates PI3K, cell polarity, and directional cell movement. J Cell Biol 167, 505–518.
Schaap P, Konijn TM, Van Haastert PJM (1984). cAMP pulses coordinate morphogenetic movement during fruiting body formation of Dictyostelium minutum. Proc Natl Acad Sci USA 81, 2122–2126.
Schaap P, Wang M (1984). The possible involvement of oscillatory cAMP signaling in multicellular morphogenesis of the cellular slime molds. Dev Biol 105, 470–478.
Schaap P, Wang M (1985). cAMP induces a transient elevation of cGMP levels during early culmination of Dictyostelium minutum. Cell Differ 16, 29–33.
Schoen CD, Schulkes CC, Arents JC, van Driel R (1996). Guanylate cyclase activity in permeabilized Dictyostelium discoideum cells. J Cell Biochem 60, 411–423.
Schulkes CC, Schoen CD, Arents JC, Van Driel R (1992). A soluble factor and GTP gamma S are required for Dictyostelium discoideum guanylate cyclase activity. Biochim Biophys Acta 1135, 73–78.
Shimomura O, Suthers HL, Bonner JT (1982). Chemical identity of the acrasin of the cellular slime mold Polysphondylium violaceum. Proc Natl Acad Sci USA 79, 7376–7379.
Sun TJ, Van Haastert PJM, Devreotes PN (1990). Surface cAMP receptors mediate multiple responses during development in Dictyostelium: evidenced by antisense mutagenesis. J Cell Biol 110, 1549–1554.
Tanabe Y, Kamimura Y, Ueda M (2018). Parallel signaling pathways regulate excitable dynamics differently to mediate pseudopod formation during eukaryotic chemotaxis. J Cell Sci 131, jcs214775.
Tesmer JJ, Sunahara RK, Johnson RA, Gosselin G, Gilman AG, Sprang SR (1999). Two-metal-Ion catalysis in adenylyl cyclase. Science 285, 756–760.
Valkema R, Van Haastert PJM (1992). Inhibition of receptor-stimulated guanylyl cyclase by intracellular calcium ions in Dictyostelium cells. Biochem Biophys Res Commun 186, 263–268.
Valkema R, Van Haastert PJM (1994). A model for cAMP-mediated cGMP response in Dictyostelium discoideum. Mol Biol Cell 5, 575–585.
Van Egmond WN (2010). Biochemical and Functional Aspects of GbpC and Other Roco Proteins in Dictyostelium discoideum. PhD Thesis. Groningen, the Netherlands: Groningen University.
Van Haastert PJM (1987). Differential effects of temperature on cAMP-induced excitation, adaptation, and deadaptation of adenylate and guanylate cyclase in Dictyostelium discoideum. J Cell Biol 105, 2301–2306.
Van Haastert PJM (2006). Analysis of signal transduction: formation of cAMP, cGMP, and Ins(1,4,5)P3 in vivo and in vitro. Methods Mol Biol 346, 369–392.
Van Haastert PJM (2020). Unified control of amoeboid pseudopod extension in multiple organisms by branched F-actin in the front and parallel F-actin/myosin in the cortex. PLoS One 15, e0243442.
van Haastert PJM (2021). Short- and long-term memory of moving amoeboid cells. PLoS One 16, e0246345.
Van Haastert PJM, De Vries MJ, Penning LC, Roovers E, Van der Kaay J, Erneux C, Van Lookeren Campagne MM (1989). Chemoattractant and guanosine 5′-[gamma-thio]triphosphate induce the accumulation of inositol 1,4,5-trisphosphate in Dictyostelium cells that are labelled with [3H]inositol by electroporation. Biochem J 258, 577–586.
Van Haastert PJM, De Wit RJ, Grijpma Y, Konijn TM (1982b). Identification of a pterin as the acrasin of the cellular slime mold Dictyostelium lacteum. Proc Natl Acad Sci USA 79, 6270–6274.
Van Haastert PJM, Van Lookeren Campagne MM, Ross FM (1982a). Altered cGMP-phosphodiesterase activity in chemotactic mutants of Dictyostelium discoideum. FEBS Lett 147, 149–152.
Varnum B, Soll DR (1984). Effects of cAMP on single cell motility in Dictyostelium. J Cell Biol 99, 1151–1155.
Veltman DM, Akar G, Bosgraaf L, Van Haastert PJM (2009a). A new set of small, extrachromosomal expression vectors for Dictyostelium discoideum. Plasmid 61, 110–118.
Veltman DM, Keizer-Gunnink I, Van Haastert PJM (2009b). An extrachromosomal, inducible expression system for Dictyostelium discoideum. Plasmid 61, 119–125.
Veltman DM, Roelofs J, Engel R, Visser AJ, Van Haastert PJM (2005). Activation of soluble guanylyl cyclase at the leading edge during Dictyostelium chemotaxis. Mol Biol Cell 16, 976–983.
Veltman DM, Van Haastert PJM (2006). Guanylyl cyclase protein and cGMP product independently control front and back of chemotaxing Dictyostelium cells. Mol Biol Cell 17, 3921–3929.
Wu L, Valkema R, Van Haastert PJM, Devreotes PN (1995). The G protein beta subunit is essential for multiple responses to chemoattractants in Dictyostelium. J Cell Biol 129, 1667–1675.
Wurster B, Schubiger K, Wick U, Gerisch G (1977). Cyclic GMP in Dictyostelium discoideum, Oscillations and pulses in response to folic acid and cyclic AMP signals. FEBS Lett 76, 141–144.
Xiong Y, Huang C-H, Iglesias PA, Devreotes PN (2010). Cells navigate with a local-excitation, global-inhibition-biased excitable network. Proc Natl Acad Sci USA 107, 17079–17086.
Zhang S, Charest PG, Firtel RA (2008). Spatiotemporal regulation of Ras activity provides directional sensing. Curr Biol 18, 1587–1593.